3-2020

Optimal control with MANF treatment of photoreceptor degeneration

Erika T. Camacho

Suzanne Lenhart

Luis A. Melara

M. Cristina Villalobos
The University of Texas Rio Grande Valley

Stephen Wirkus

Recommended Citation

Erika T Camacho, Suzanne Lenhart, Luis A Melara, M Cristina Villalobos, Stephen Wirkus, Optimal control with MANF treatment of photoreceptor degeneration, Mathematical Medicine and Biology: A Journal of the IMA, Volume 37, Issue 1, March 2020, Pages 1–21, https://doi.org/10.1093/imammb/dqz003

Mathematical Medicine and Biology: A Journal of the IMA (2020) **37**, 1–21
doi:10.1093/imammb/dqz003
Advance Access publication on 27 February 2019

Optimal control with MANF treatment of photoreceptor degeneration

Erika T. Camacho*
School of Mathematical & Natural Sciences, Arizona State University, Phoenix, AZ 85306, USA
*Corresponding author. E-mail: erika.camacho@asu.edu

Suzanne Lenhart
Department of Mathematics, University of Tennessee, Knoxville, TN 37996-1320, USA

Luis A. Melara
Department of Mathematics, Shippensburg University, Shippensburg, PA 17257, USA

M. Cristina Villalobos
School of Mathematical and Statistical Sciences, The University of Texas Rio Grande Valley, Edinburg, TX 78539, USA

and

Stephen Wirkus
School of Mathematical & Natural Sciences, Arizona State University, Phoenix, AZ 85306, USA

[Received on 26 June 2018; revised on 1 February 2019; accepted on 3 February 2019]

People afflicted with diseases such as retinitis pigmentosa and age-related macular degeneration experience a decline in vision due to photoreceptor degeneration, which is currently unstoppable and irreversible. Currently there is no cure for diseases linked to photoreceptor degeneration. Recent experimental work showed that mesencephalic astrocyte-derived neurotrophic factor (MANF) can reduce neuron death and, in particular, photoreceptor death by reducing the number of cells that undergo apoptosis. In this work, we build on an existing system of ordinary differential equations that represent photoreceptor interactions and incorporate MANF treatment for three experimental mouse models having undergone varying degrees of photoreceptor degeneration. Using MANF treatment levels as controls, we investigate optimal control results in the three mouse models. In addition, our numerical solutions match the experimentally observed surviving percentage of photoreceptors and our uncertainty and sensitivity analysis identifies significant parameters in the math model both with and without MANF treatment.

Keywords: optimal control, mesencephalic astrocyte-derived neurotrophic factor, photoreceptor degeneration, apoptosis, model of ordinary differential equations.

1. Introduction

1.1 *Background of photoreceptor degeneration*

The most common forms of blindness in the world are treatable. In 2015, the World Health Organization (WHO) estimated that approximately 253 million people in the world are vision impaired with 36 million blind and 217 million suffering from moderate to severe vision impairment. Over 80% of all vision impairment can be avoided, prevented or cured except for blindness related to photoreceptor degeneration (World Health Organization Vision Impairment and Blindness, 2017). Avoidable blindness results from conditions that can be prevented or controlled if knowledge and interventions are available

and applied in a timely manner or if the sight loss condition is successfully treated in order to restore sight (e.g. cataract). While tremendous improvements have been made in some areas of blindness prevention and control, trends in an ageing and growing population coupled with the increase in myopia and diabetic retinopathy are counteracting the decrease in blindness catalysed by the target goal of the WHO (to decrease blindness by 25% from 2010 to 2020). The global cost of blindness is projected to double by 2020 from the $80 million per year spent today (Bourne *et al.*, 2017; World Health Organization Vision Impairment and Blindness, 2017; World Health Organization Vision Media Center, 2018). Blindness is predicted to increase threefold by 2050 (from 38.5 million people in 2020 to 115 million in 2050) (Pizzarello *et al.*, 2004).

However, blindness due to degeneration of the photoreceptors still has no cure. The most common forms of blindness caused by photoreceptor degeneration include age-related macular degeneration (AMD) and untreated retina detachment (due to trauma). Photoreceptor degeneration also occurs in retinitis pigmentosa (RP), which is the leading cause of hereditary blindness. RP is a heterogeneous group of diseases that typically manifests itself between adolescence and early adulthood, affecting approximately 1 in 4000 individuals (Besharse & Bok, 2011; Mohand-Said *et al.*, 2001; Shintani *et al.*, 2009). To date, more than 45 gene mutations have been identified, each of which causes RP, and all are seen to be present in the rod photoreceptor or the retinal pigment epithelium (RPE) (Hamel, 2006; Phelan & Bok, 2000). These genes are mostly responsible for encoding proteins involved in the phototransduction cascade, the photoreceptor structure or the visual cycle (Busskamp *et al.*, 2010; Chalmel *et al.*, 2007; Hartong *et al.*, 2006; Malanson & Lem, 2009; Shen *et al.*, 2005; Shintani *et al.*, 2009). Even in members of the same family carrying the exact same mutation, the age of onset, the disease progression and the characteristics of RP vary dramatically among patients (Besharse & Bok, 2011; Shen *et al.*, 2005; Wong, 1997). Rod death is a hallmark of the disease and results in night blindness yet preventing degeneration of the rods has proven difficult given the myriad of mutations that cause the disease. However, in spite of the wide range of mutations that ultimately result in rod degeneration, the degeneration of the healthy cones inevitably follows. Since it is the cone photoreceptors that are responsible for day vision, colour vision and accuity, it is this secondary death wave (in which the cones die) that has generated a tremendous amount of research (Besharse & Bok, 2011; Hartong *et al.*, 2006; Shen *et al.*, 2005; Shintani *et al.*, 2009). The secondary death wave typically begins when approximately 95% of the rods have died (Camacho *et al.*, 2016a,b). A recent discovery found that the rods release a protein, the rod-derived cone viability factor (RdCVF), that facilitates glucose uptake by the cones, and therapies involving this factor hold promise (Aït-Ali *et al.*, 2015; Léveillard & Sahel, 2010; Sahel, 2005; Yang *et al.*, 2009).

In terms of sight, light passes through the cornea, pupil and lens and ultimately hits the retina in the back of the eye. This is where phototransduction begins; the light sensitive rod and cone photoreceptors in the retina receive the light impulse and begin the vision process to transmit the signal to the brain. The rods and cones are separate entities in close proximity in the retina and receive their essential supplies from the choroid via the adjacent RPE. Thus, it is important to understand the interactions within these specialized cells that form a functional unit that is critical for sight (Strauss, 2005). The visual cycle and process by which a light signal is received by the eye and transmitted to the brain is well understood (Keener & Sneyd, 2008; Oyster, 1999). In order to be sensitive to light signals and the frequency with which light is received, the photoreceptors undergo a tremendous amount of stress on a daily basis. The rods and cones are equipped to deal with this stress through periodic shedding at the distal tip (near the RPE) and continuous renewal at the basal end of their outer segments (OS), which are made up of discs (Bok, 1985; Hendrickson, 2008; David, May, 2002). Roughly 10% of each OS is shed each day by all the cones and rods and these are then phagocytized by the adjacent RPE. The RPE

also facilitates renewal as it delivers essential proteins and growth factors to the rods and cones. The balance of shed and renewed discs ensures that the overall length of the OS remains roughly constant over a day. Neural degeneration of the photoreceptors that typically results from genetic defects and mutations (such as in RP) are implicated in disturbances of the shedding and renewal processes resulting in abnormal photoreceptor OS length and thus promoting the complete disappearance of the rods and cones (Mohand-Said *et al.*, 2001; Pallikaris *et al.*, 2003). Changes can occur either inside or outside a cell of a multicellular organism that trigger the cell to self-destruct. This is termed apoptosis and is sometimes referred to as programmed cell death. Additionally, apoptosis is observed to be another process of photoreceptor death in RP and other diseases in which photoreceptor death occurs (Kernan *et al.*, 2007).

1.2 *Treatment options and mesencephalic astrocyte-derived neurotrophic factor*

There is no method of stopping photoreceptor death. Experimentalists have been undertaking a range of methods that attempt to stop photoreceptor degeneration. Non-invasive methods that have been pursued involve supplementation, e.g. with vitamin A and high doses of omega-3 fatty acid (including Docosahexaenoic acid (DHA)) (Berson, 1993). Gene therapy has recently gained much attention as researchers attempt to correct mutated genetic material in the rods with the insertion of healthy genes. In photoreceptor degeneration caused by RP, treatments that do not target a specific mutation have more promise given the heterogeneity of this inherited disease. Stem cell therapy is also being explored to see if stem cells injected into the retina can be persuaded to differentiate into retinal cells. They would then have the potential to replace damaged or missing retinal cells, which is very promising since retinal cells are not born in a mature retina and are thus not replaced by the body after they have died. One common mechanism of photoreceptor cell death in the above maladies is apoptosis, and researchers have pursued methods to better understand and possibly prevent apoptosis.

In 2003, Petrova *et al.* (2004) discovered the secreted protein mesencephalic astrocyte-derived neurotrophic factor (MANF). In the central nervous system, astrocytes and neurons interact functionally to mediate processes such as neuroprotection. An important group of secreted proteins, these neurotrophic factors help regulate the life and death of neurons. Astrocytes produce neurotrophic molecules that affect neuronal development and survival, among other things, and the astrocyte-derived MANF is part of a new class of therapeutics specifically used to treat diseases of the central nervous system. A key benefit of MANF is that it can prevent apoptosis regardless of the cause and therefore potentially may be able to cure diseases affecting neurons, such as RP or Parkinson's disease, without knowing the fundamental cause of this degeneration. Neurotrophic factors, including MANF, prevent apoptosis and regulate the number of neurons innervating the target tissue (Lindholm & Saarma, 2010).

In 2016, Neves *et al.* (2016) demonstrated that MANF prevents apoptosis in the photoreceptors of three different mouse models (i.e. three types of mice, each strain bred for a certain genetic makeup). As apoptosis is the cause of a large number of photoreceptor deaths in AMD, RP and untreated retina detachment, this finding has potential for significant impact in preventing photoreceptor degeneration. While the experiments showed remarkable results in prevention of photoreceptor death due to genetic and non-genetic factors, MANF did not prevent all of the photoreceptors from degenerating. In addition, possible effects of overtreatment have not been explored systematically. Thus, it is important for researchers to investigate alternative treatments or improve existing ones that target other aspects of photoreceptor apoptosis and degeneration.

In this paper, we extend the mathematical model in Camacho *et al.* (2010), Camacho *et al.* (2016b), Camacho & Wirkus (2013) and Camacho *et al.* (2014), which illustrates the physical interaction of

the photoreceptors and their trophic pool containing nutrients, metabolites, glucose, water, ions and other essential growth factors. In Camacho *et al.* (2014), we considered drug treatment of RP through the RdCVF factor where our numerical results agreed with experimental results in mice showing 40% cone rescue effect in a rod free retina. Now, we introduce drug treatment through the MANF factor in the three photoreceptor degeneration mouse models in Neves *et al.* (2016) having varying degrees of retinal degeneration (two models due to light exposure with different levels of photosensitivity and the third model due to RP) and consider MANF as the control variable. In doing so, we introduce apoptosis to the system. Our goal is to study the influence of MANF on preventing photoreceptor death through a mathematical model with optimal control techniques and make comparisons with experimental results given in Neves *et al.* (2016). Section 2 introduces the new mathematical model along with the optimal control formulation, and in Section 3 the first-order necessary conditions of the optimal control problem are given. In Section 4, we discuss numerical results via sensitivity analysis with partial rank correlation coefficients (PRCC) of parameter values used in the mathematical model, and follow-up with a discussion of results in the solution of the optimal control problem for all three mouse models. Finally, Section 5 gives a brief discussion of the conclusions.

2. Mathematical model

In this section, we initially introduce the system of differential equations governing the photoreceptor interactions, followed by a discussion of the optimal control problem on the three mouse models. The mathematical models in Camacho *et al.* (2010, 2016b) and Camacho & Wirkus (2013) describe the interactions between the nutrient-containing trophic pool and the three populations of photoreceptors: the cones and two types of rods, where the rods are divided into two populations based on their phenotype. All three photoreceptor populations and the trophic pool are functions of time t and defined as follows:

$$\begin{aligned} R_n(t) &: \quad \text{population of normal rods,} \\ R_m(t) &: \quad \text{population of mutated rods,} \\ C(t) &: \quad \text{population of cones and} \\ T(t) &: \quad \text{trophic pool (RPE).} \end{aligned}$$

Here we consider R_m to represent those rods that have begun to express the RP gene mutation and thus have had some aspect of their functionality compromised Camacho & Wirkus (2013). For the three photoreceptor populations, we consider the units to be 'number of cells'. Fractions of a cell are interpreted as the photoreceptor outer segment discs and as the nutrients (such as growth factors, metabolites, ions and water) for the trophic pool (Frasson *et al.*, 1999; LaVail *et al.*, 1998; Li *et al.*, 2010; Longbottom *et al.*, 2009; Murakami *et al.*, 2008; Strauss, 2005; Wenzel *et al.*, 2005). Because the trophic pool is mediated by the RPE, we view the RPE cells as a proxy for the trophic pool (Camacho *et al.*, 2010, 2016a,b; Camacho & Wirkus, 2013). The system of differential equations modelling these interactions is given by

$$\dot{R}_n = R_n(a_n T - \mu_n - m) \tag{1}$$

$$\dot{R}_m = R_m(a_m T - \mu_m) + mR_n \tag{2}$$

$$\dot{C} = C(a_c T - \mu_c + d_n R_n + d_m R_m) \tag{3}$$

$$\dot{T} = T(\Gamma - kT - \beta_n R_n - \beta_m R_m - \gamma C), \tag{4}$$

where the parameters are nonnegative and define various physiological mechanisms and processes; see Table 1. Briefly, the a_i terms represent renewal rates, m represents the rate of phenotypic expression of the mutation, d_i represent the one-way help provided by the rods to the cones, Γ is the inflow rate of nutrients into the trophic pool, k limits the capacity of this inflow and β_i, γ are the removal of nutrients by rods and cones from the trophic pool. Additionally, the product of T with a photoreceptor population signifies the consumption of nutrients by the respective populations. We note the use of the parameters μ_n, μ_m and μ_c, which describe decay rates in the respective populations of the normal rods, mutated rods and the cones, and which will be further described below. A thorough analysis of the equilibrium in (1)–(4) and their stability was done in Camacho & Wirkus (2013). In particular, equilibria of the form (R_n^*, R_m^*, C^*, T^*) were found with only one equilibrium being stable for any given set of parameters in the physiologically observed parameter regions. Two steady-state values that occur for the parameters in the three photoreceptor degeneration mouse models are $R_n^* + R_m^* \neq 0$, $C^* \neq 0$, $T^* \neq 0$ (where both rods and cones survive) and $R_n^* = R_m^* = C^* = 0$, $T^* \neq 0$ (where rods and cones both die).

Now we introduce apoptosis into the system of differential equations. Hence, the parameters μ_n, μ_m and μ_c in equations 13 are rewritten to explicitly include contributions from shedding (replaced by renewal) and apoptosis (permanent loss):

$$\mu_n = \mu_{ns} + \mu_{na} \tag{5}$$

$$\mu_m = \mu_{ms} + \mu_{ma} \tag{6}$$

$$\mu_c = \mu_{cs} + \mu_{ca}, \tag{7}$$

where, e.g. μ_{ns} describes the shedding rate of the normal rods, and μ_{na} describes the apoptosis rate of the normal rods. Substituting (5)–(7) into (1)–(4) yields the new system of differential equations for our mathematical model under the study:

$$\dot{R}_n = R_n(a_n T - \mu_{ns} - m) - \mu_{na} R_n \tag{8}$$

$$\dot{R}_m = R_m(a_m T - \mu_{ms}) + mR_n - \mu_{ma} R_m \tag{9}$$

$$\dot{C} = C(a_c T - \mu_{cs} + d_n R_n + d_m R_m) - \mu_{ca} C \tag{10}$$

$$\dot{T} = T(\Gamma - kT - \beta_n R_n - \beta_m R_m - \gamma C). \tag{11}$$

2.1 *Optimal control problem formulation*

Based on our previous discussion on experimental results conducted by Neves *et al.* (2016), treatment with MANF prevents apoptosis. Thus, we use optimal control theory to find treatment strategies applying MANF to three mouse models with varying degrees of retinal degeneration. We will call the solutions of our system as the states, R_n, R_m, C and T. The control variable $u \equiv u(t)$ describes

TABLE 1 *Parameter value ranges for system (12)-(15); the values were calibrated for a mouse model in Camacho et al. (2016b). The variables C, R_n, R_m, T represent populations of cells*

Parameter	Description	Units	Source
$\Gamma \in [4.55, 5.21]$	Total inflow rate into the trophic factor T	days^{-1}	Camacho *et al.* (2016b); Guérin *et al.* (1993)
$k \in [1.95, 16.0] \times 10^{-4}$	Limiting capacity of trophic factors	$(T\cdot\text{days})^{-1}$	Camacho *et al.* (2016b); Guérin *et al.* (1993)
$\beta_n \in [2.09, 3.88] \times 10^{-8}$	Constant per cell rate at which R_n withdraws T	$(R_n\cdot\text{days})^{-1}$	Camacho *et al.* (2016b); Guérin *et al.* (1993)
$\beta_m \in [2.44, 3.78] \times 10^{-8}$	Constant per cell rate at which R_m withdraws T	$(R_m\cdot\text{days})^{-1}$	Camacho *et al.* (2016b); Guérin *et al.* (1993)
$\gamma \in [3.5, 18.1] \times 10^{-6}$	Constant per cell rate at which C withdraws T	$(C\cdot\text{days})^{-1}$	Camacho *et al.* (2016b); Guérin *et al.* (1993)
$m \in [1.1, 466] \times 10^{-3}$	Rate of R_n losing significant functionality	days^{-1}	Camacho *et al.* (2016b)
$d_n \in [3.28, 5.47] \times 10^{-9}$	Constant per cell rate at which R_n helps C	$(C\cdot\text{days})^{-1}$	Guérin *et al.* (1993); Léveillard *et al.* (2004)
$d_m \in [1.01, 3.79] \times 10^{-9}$	Constant per cell rate at which R_m helps C	$(C\cdot\text{days})^{-1}$	Léveillard *et al.* (2004)
$\mu_{ns} \in [.0912, .1075]$	OS shedding rate of R_n	days^{-1}	Camacho *et al.* (2016b); Murakami *et al.* (2012); Young (1971)
$\mu_{ms} \in [.0995, .119]$	OS shedding rate of R_m	days^{-1}	Murakami *et al.* (2012)
$\mu_{cs} \in [.120, .125]$	OS shedding rate of C	days^{-1}	Jonnal *et al.* (2010); Murakami *et al.* (2012); Young (1971)
$a_n \in [4.297, 5.617] \times 10^{-6}$	Per cell normal rod renewal rate	$(T\cdot\text{days})^{-1}$	Camacho *et al.* (2016b); Guérin *et al.* (1993)
$a_m \in [1.831, 6.101] \times 10^{-6}$	Per cell mutated rod renewal rate	$(T\cdot\text{days})^{-1}$	Camacho *et al.* (2016b); Guérin *et al.* (1993)
$a_c \in [4.383, 5.239] \times 10^{-6}$	Per cell cone renewal rate	$(T\cdot\text{days})^{-1}$	Camacho *et al.* (2016b); Guérin *et al.* (1993)
$\mu_{na}, \mu_{ma}, \mu_{ca} \in [0.63, 0.69]$	Per cell photoreceptor apoptosis rate, BALB/cJ mouse	days^{-1}	Matsumoto *et al.* (2014); Neves *et al.* (2016); Wenzel *et al.* (2001)
$\mu_{na}, \mu_{ma}, \mu_{ca} \in [0.32, 0.39]$	Per cell photoreceptor apoptosis rate, C57BL/6 mouse	days^{-1}	Matsumoto *et al.* (2014); Neves *et al.* (2016); Wenzel *et al.* (2001)
$\mu_{na}, \mu_{ma} \in [0.14, 0.31]$	Per cell rod apoptosis rate, $Pde6b^{Rd1}$ mouse	days^{-1}	Neves *et al.* (2016); Punzo *et al.* (Jan, 2009)
$\mu_{ca} \in [0, 0.01]$	Per cell cone apoptosis rate, $Pde6b^{Rd1}$ mouse	days^{-1}	Neves *et al.* (2016); Punzo *et al.* (Jan, 2009)

the percentage of decrease in apoptosis from a corresponding level of the MANF treatment and is incorporated into the state equations to affect apoptosis in the three photoreceptor populations:

$$\dot{R}_n = R_n(a_n T - \mu_{ns} - m) - \mu_{na}(1-u)R_n \tag{12}$$

$$\dot{R}_m = R_m(a_m T - \mu_{ms}) + mR_n - \mu_{ma}(1-u)R_m \tag{13}$$

$$\dot{C} = C(a_c T - \mu_{cs} + d_n R_n + d_m R_m) - \mu_{ca}(1-u)C \tag{14}$$

$$\dot{T} = T(\Gamma - kT - \beta_n R_n - \beta_m R_m - \gamma C). \tag{15}$$

We note that the control variable u is dimensionless; a value of u represents the percentage of decreasing effect on apoptosis due to the corresponding dosage while $u = 0$ represents either completely ineffective treatment or no applied treatment. To achieve high population levels of rods and cones while not applying excessive treatment, we seek to maximize the objective functional

$$J(u) = \int_0^{t_f} \left(\left(\alpha_1 R_n + \alpha_2 R_m + \alpha_3 C\right) - \varepsilon \frac{u^2}{2} \right) \mathrm{d}t, \tag{16}$$

where the first terms represent a weighted sum of the rods and cones. The positive weight ε represents the importance of applying moderate treatment. The nonnegative weights α_1, α_2 and α_3 represent the importance of maximizing the populations of rods (R_n and R_m, respectively) and cones. Experiments involving MANF are relatively new and we have not found any that discuss toxicity of MANF. However, we assume that high levels of MANF will result in some level of toxicity and thus we use u^2, but this term will be small in relationship to the other terms since $0 < u < 1$. The toxicity is assumed to be a nonlinear function of the control and we choose a simple nonlinear function with a weight of $\epsilon/2$ with the division by 2 done for mathematical convenience. We define the set of controls U as

$$U = \left\{ u \mid u \text{ is measurable, } u_{min} \le u(t) \le u_{max}, \ t \in [0, t_f] \right\}, \tag{17}$$

with $u_{min} \ge 0$ and $u_{max} < 1$. Note that since the control u is bounded and the corresponding states are bounded in the time interval, then the objective functional $J(u)$ is bounded over the controls u in the control set U (Lenhart & Workman, 2007).

Thus, the optimal control problem is to find u^* satisfying equations (12)–(15) such that

$$J(u^*) = \sup_u J(u). \tag{18}$$

The parameter value ranges for the optimal control problem are given in Table 1 and obtained either from the literature or from parameter estimation via inverse problem methodology (Camacho *et al.*, 2016b). Details of the origin of these parameter values can be found in Camacho *et al.* (2016b) and the references therein. The initial values for rods, cones and trophic pool in the RP mouse model $Pde6b^{Rd1}$ are taken as $R_n(0) = 3 \times 10^6$, $R_m(0) = 0.6 \times 10^6$, $C(0) = 0.18 \times 10^6$, $T(0) = 8400$ (Camacho *et al.*, 2016b). For the non-RP mouse models BALB/cJ and C57BL/6, $R_n(0) = 3.6 \times 10^6$ and $R_m(0) = 0$. The specific parameter values for each mouse model are given in Section 4 since they are dependent on the particular photoreceptor degeneration mouse model under consideration.

3. First-order necessary conditions

To use Pontryagin's maximum principle to solve the optimal control problem, we first define the Hamiltonian H as

$$\begin{aligned} H &= (\alpha_1 R_n + \alpha_2 R_m + \alpha_3 C) - \varepsilon \frac{u^2}{2} \\ &\quad + \lambda_1\big(R_n(a_n T - \mu_{ns} - m) - \mu_{na}(1-u)R_n\big) \\ &\quad + \lambda_2\big(R_m(a_m T - \mu_{ms}) + mR_n - \mu_{ma}(1-u)R_m\big) \\ &\quad + \lambda_3\big(C(a_c T - \mu_{cs} + d_n R_n + d_m R_m) - \mu_{ca}(1-u)C\big) \\ &\quad + \lambda_4\big(T(\Gamma - kT - \beta_n R_n - \beta_m R_m - \gamma C)\big), \end{aligned} \tag{19}$$

where $(\lambda_1, \lambda_2, \lambda_3, \lambda_4)$ are the adjoint functions of time t. The state variables R_n, R_m, T and C and the controls are *a priori* bounded on the time interval $[0, t_f]$, and the structure of the differential equation system (12)–(15) gives the uniform boundedness of the derivatives of the state variables. These bounds and the concavity of the functional J with respect to the control u are enough to guarantee the existence of an optimal control. Then for an optimal control and corresponding states, we can apply Pontryagin's maximum principle.

THEOREM 1 If u^* and R_n^*, R_m^*, C^*, T^* are optimal for problem (18), then there exist piecewise differentiable adjoint functions $\lambda_i : [0, t_f] \to \mathbb{R}$ for $i = 1, \ldots, 4$ such that the adjoint equations are

$$\frac{\mathrm{d}\lambda_1}{\mathrm{d}t} = -\frac{\partial H}{\partial R_n} = -\lambda_1\left(a_n T - m - (1-u)\mu_{na} - \mu_{ns}\right) - \alpha_1 - \lambda_3 d_n C - \lambda_2 m + \lambda_4 \beta_n T \tag{20}$$

$$\frac{\mathrm{d}\lambda_2}{\mathrm{d}t} = -\frac{\partial H}{\partial R_m} = -\lambda_2\left(a_m T - (1-u)\mu_{ma} - \mu_{ms}\right) - \alpha_2 - \lambda_3 d_m C + \lambda_4 \beta_m T \tag{21}$$

$$\frac{\mathrm{d}\lambda_3}{\mathrm{d}t} = -\frac{\partial H}{\partial C} = -\lambda_3\left(a_c T - (1-u)\mu_{ca} - \mu_{cs} + d_m R_m + d_n R_n\right) - \alpha_3 + \lambda_4 \gamma T \tag{22}$$

$$\frac{\mathrm{d}\lambda_4}{\mathrm{d}t} = -\frac{\partial H}{\partial T} = -C\lambda_3 a_c - \lambda_2 a_m R_m - \lambda_1 a_n R_n - \lambda_4\left(\Gamma - \gamma C - 2kT - \beta_m R_m - \beta_n R_n\right), \tag{23}$$

with transversality boundary conditions $\lambda_i(t_f) = 0$ for $i = 1, 2, 3, 4$. The characterization for this optimal control u^* is given by

$$u^* = \min\left\{u_{max}, \max\left\{u_{min}, \frac{\lambda_1 \mu_{na} R_n + \lambda_2 \mu_{ma} R_m + \lambda_3 \mu_{ca} C}{\epsilon}\right\}\right\}. \tag{24}$$

We note that the characterization of u^* depends on the three apoptosis rates, the population of rods and cones and three adjoint functions. Hence, the characterization of u^* and corresponding state and adjoint equations will be numerically computed.

4. Numerical results and discussion

Recent experimental work by Neves *et al.* (2016) demonstrates that MANF prevents apoptosis in the photoreceptors of mice. Utilizing the experimental results from three photoreceptor degeneration mouse models in Neves *et al.* (2016), we compare the results and outputs of our mathematical model, both with and without control, to clarify the key role of optimal control with MANF treatment. We first conduct an uncertainty analysis and sensitivity analysis on the significance of the parameters, and then present results on the optimal control problem.

The first two mouse models (the highly light-sensitive BALB/cJ and the normal C57BL/6 mouse models) do not naturally exhibit photoreceptor degeneration; however, both undergo photoreceptor degeneration with overexposure to high intensities of light. The light sensitive BALB/cJ strain lacks the protective variant of the Rpe65 allele which causes the photoreceptors in mice to be very susceptible to light induced retinal damage as opposed to the C57BL/6 strain which has the allele and thus retinal damage requires high exposure to light (Neves *et al.*, 2016). The third mouse model $Pde6b^{Rd1}$ has manifested RP. Utilizing these three mouse models allows us to mathematically analyse the effect of MANF treatment on both photoreceptor degeneration due to (1) RP via the $Pde6b^{Rd1}$ mouse model, and (2) reactive oxidative species (ROS), a natural by-product of light absorption which leads to accumulation of photo toxic products via a slow photoreceptor degeneration in the C57BL/6 mouse model and a fast degeneration in the BALB/cJ mouse model.

The results of Neves et al. refer to the percentage of photoreceptors present after treatment and as such we consider the % photoreceptors surviving as

$$\frac{\text{number of photoreceptors surviving with MANF}}{\text{initial number of photoreceptors}} = \frac{(\hat{R}_n + \hat{R}_m + \hat{C})(t_f)}{(\hat{R}_n + \hat{R}_m + \hat{C})(t_0)} \tag{25}$$

$$\frac{\text{number of photoreceptors surviving without MANF}}{\text{initial number of photoreceptors}} = \frac{(R_n + R_m + C)(t_f)}{(R_n + R_m + C)(t_0)}, \tag{26}$$

where $\hat{R}_n$, $\hat{R}_m$ and $\hat{C}$ represent the amount of photoreceptors present at time t when optimal control is applied. Thus, this formula provides the percentage of photoreceptors present after treatment. In each of the MANF experiments, the results are presented as nuclei of the photoreceptors alive vs. in the process of dying (Terminal deoxynucleotidyl transferase dUTP nick end labeling (TUNEL) positive) in a representative cross-section that allowed the researchers to count cell nuclei as well as measure the thickness of the outer nuclear layer and inner nuclear layer (Neves *et al.*, 2016). We extend these ratios to the full mouse retina as done experimentally in Neves *et al.* (2016) to extract the number of photoreceptors in the full retina and compare our results accordingly.

The parameter values used for the plots in the BALB/cJ, C57BL/6 and $Pde6b^{Rd1}$ mouse models are

$$\begin{aligned} &\mu_{ns} = 0.103,\ \mu_{cs} = 0.119,\ \Gamma = 4.93,\ a_n = 4.909 \times 10^{-6}, \\ &a_c = 5.12 \times 10^{-6},\ \beta_n = 2.50 \times 10^{-8},\ d_n = 3.4 \times 10^{-9},\ \gamma = 4 \times 10^{-6}. \end{aligned} \tag{27}$$

Additionally, in the BALB/cJ and C57BL models we set

$$\begin{aligned} &k = 2 \times 10^{-4},\ d_m = d_n,\ \mu_{ms} = \mu_{ns},\ a_m = a_n,\ \beta_m = \beta_n,\ m = 0, \\ &\alpha_1 = \alpha_2 = 5,\ \epsilon = 1; \alpha_3 = 4(\text{BALB/cJ}), \alpha_3 = 2(\text{C57BL/6}) \end{aligned} \tag{28}$$

and in the $Pde6b^{Rd1}$ model we set

$$k = 2.25 \times 10^{-4}, d_m = 6.91 \times 10^{-9}, \beta_m = 2.29 \times 10^{-8}, \mu_{ms} = 0.0994,$$
$$a_m = 5.24 \times 10^{-6}, m = 3.68 \times 10^{-1}, \alpha_1 = \alpha_2 = 15, \alpha_3 = 10, \epsilon = 1 \quad (29)$$

for the simulations (Camacho *et al.*, 2016b). For the first two mouse models without a mutation, BALB/cJ and C57BL/6, we set $m = 0$ in (28) whereas for the mouse model $Pde6b^{Rd1}$, which has a mutation that causes RP, we have $m > 0$ in (29). Previous work shows that RP mouse models have lower nutrient availability which is represented by the slightly larger k-value (Camacho *et al.*, 2016b; Camacho & Wirkus, 2013). In the absence of treatment, the experiments in Neves *et al.* (2016) show death of the photoreceptors over the given time frame of 2 days or 5 days with the amount of photoreceptor death dependent on the particular mouse model. The above parameter sets give values in the range of the experimental results of photoreceptor death in Neves *et al.* (2016) in the absence of control (i.e. absence of treatment).

4.1 *Sensitivity analysis*

While experiments have shown that MANF can significantly decrease apoptosis in multiple mouse models, previous experimental work in photoreceptor degeneration has shown other mechanisms are important in affecting photoreceptor survival including balanced energy between consumption and uptake; sufficient nutrients, glucose, RdCVF and neuroprotective factors (such as Pigment epithelium-derived factor (PEDF), basic fibroblast growth factor (bFGF) and Ciliary neurotrophic factor (CNTF)); oxidative stress; and disruptions in the rapamycin (mTOR) pathway regulating nutrient demand, and supply from the RPE (Camacho *et al.*, 2016b; Li *et al.*, 2010; Mohand-Saïd *et al.*, 1998; Mohand-Said *et al.*, 2000, 2001; Punzo *et al.*, Jan 2009, 2012; Strauss, 2005). Recently, research in the coexistence of rods and cones has indicated that cellular metabolism associated with shedding and renewal as well as aerobic glycolysis is critical in maintaining photoreceptors alive (Camacho *et al.*, 2016a). Thus, our goal is to utilize the results of this uncertainty analysis and sensitivity analysis to better understand the relative role of MANF in preventing photoreceptor death and suggest potential multifaceted treatment strategies for preventing photoreceptor death (and halting blindness) and examine which processes (defined by the parameters in our mathematical model) have the most significant effect in the presence of treatment with MANF and in the absence of such treatment.

In the cases of no treatment and of optimal treatment with MANF, we examine the significance of the various parameters on the output, defined by total photoreceptor population ($R_n + R_m + C$) at the final time values used in the three mouse model experiments. In examining the sensitivity analysis of the output to its parameters (including the initial conditions), we used the latin hypercube sampling (LHS) with PRCC method described in Marino *et al.* (2008). We have a total of four initial conditions for the four state variables and 17 parameters; see Table 1 for a description of the parameters. Together, each of the parameters has a range of reasonable values that contain their baseline values given in (27)–(29). For the apoptosis rates, we consider the range to be the baseline value $\pm 10\%$ with the baseline values of $\mu_{na} = \mu_{ma} = \mu_{ca} = 0.65$ for the BALB/cJ mouse model, $\mu_{na} = \mu_{ma} = \mu_{ca} = 0.35$ for the C57BL/6 mouse model and $\mu_{na} = \mu_{ma} = 0.22$, $\mu_{ca} = 0$ for the $Pde6b^{Rd1}$ mouse model. These numerical values are based on experimental observations of apoptosis in Neves *et al.* (2016), Punzo *et al.* (Jan, 2009) and Wenzel *et al.* (2001); death by apoptosis was nearly twice as much in the light-sensitive BALB/cJ as in C57BL/6 (0.65 vs. 0.35). In the RP model, $Pde6b^{Rd1}$, the value (0.22) is chosen because the mouse

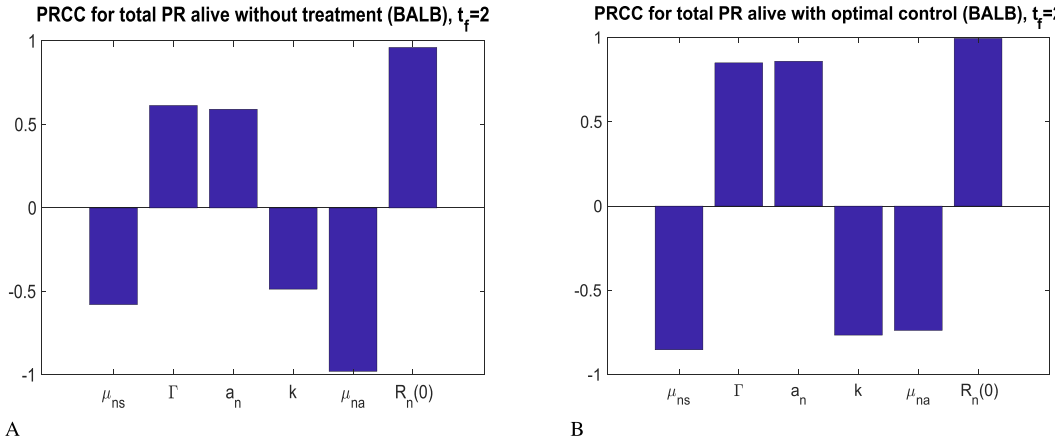

FIG. 1. **PRCC plots without and with optimal control for the BALB/cJ mouse model.** The panels, A and B, are the PRCC values for the total photoreceptor (PR) populations without and with optimal MANF treatment, respectively. In comparing the results without control (A) vs. with optimal control (B), there are no differences in the significant parameters present. However, with treatment, the role of apoptosis (μ_{na}) has a decreased magnitude while the role of shedding and renewing OS (μ_{ns} and a_n, respectively) together with the nutrient supply and limiting characteristics of the nutrients (Γ and k, respectively) has an increased magnitude.

is in days 7–12 of degeneration and this is the approximate apoptosis rate for rods over that period (Camacho *et al.*, 2016b; Neves *et al.*, 2016; Punzo *et al.*, Jan, 2009). Using these ranges we perform LHS. All parameters satisfied the monotonicity conditions of the output as required for PRCC analysis for all three mice models. For our PRCC analysis, we consider significant to be those parameters that result in a PRCC value larger than 0.4 in absolute value with p-values less than 0.05. All p-values of the parameters in Figs 1–3 presented here are less than 10^{-6}.

Figures 1–3 demonstrate the significant effect that MANF has on apoptosis and suggests additional parameters that can be targeted to prevent photoreceptor death. The parameters in our model define various physiological processes and mechanisms (as described in Table 1) and thus parameters that have a significant effect in the population of photoreceptors as illustrated by our sensitivity analysis results may suggest potential therapies that are known to affect the processes/mechanisms represented by these parameters in Figs 1–3 and summarized in Table 2. The characteristics of the mouse models and the methods of the experiments in Neves *et al.* (2016) that were used in this work are summarized in the first two rows of Table 3. In all of the results, increasing the initial number of rods significantly affects the overall photoreceptor population. However this significance is not changed with MANF treatment. We note that while retinal transplants or stem cells may be able to affect this number, using them as potential treatments to prevent photoreceptor degeneration is still unclear as retinal transplants' success has been very limited and mixed and the retina stem cell research is still in its infancy with no differentiation of retina photoreceptors having been achieved to date. Currently there are no treatments that can alter in a positive way the number of rods or cones as there is no spontaneous regeneration of photoreceptors in a mature retina. For this reason we will limit our discussion of our sensitivity analysis results to other significant parameters. At this point it is worth mentioning that the large number of rods (3.6×10^6) compared with the cones (0.18×10^6) in the mouse retina eliminates the possibility of any cone process playing a significant role in the total photoreceptor population.

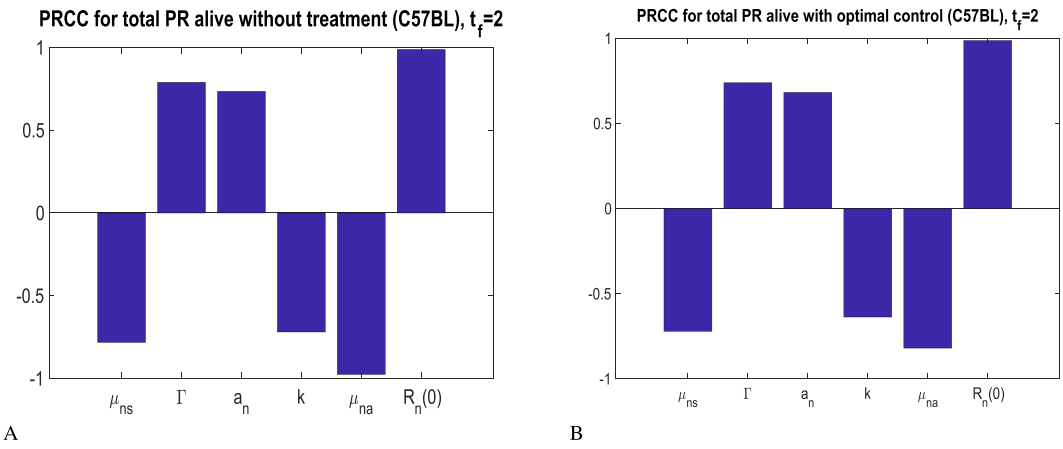

FIG. 2. **PRCC plots without and with optimal control for the C57BL/6 mouse model.** The panels, A and B, are the PRCC values for the total PR populations without and with optimal MANF treatment, respectively. In comparing the results without control (A) vs. with optimal control (B), there are no differences in the significant parameters present. The magnitude of apoptosis (μ_{na}) is lessened with treatment. However, the relative magnitude of the remaining parameters has not changed. When degeneration in a non-diseased retina is slow, MANF treatment only affects the magnitude of apoptosis, unlike in the BALB/cJ mouse model, even though the same treatments would work on both types of photoreceptor degeneration.

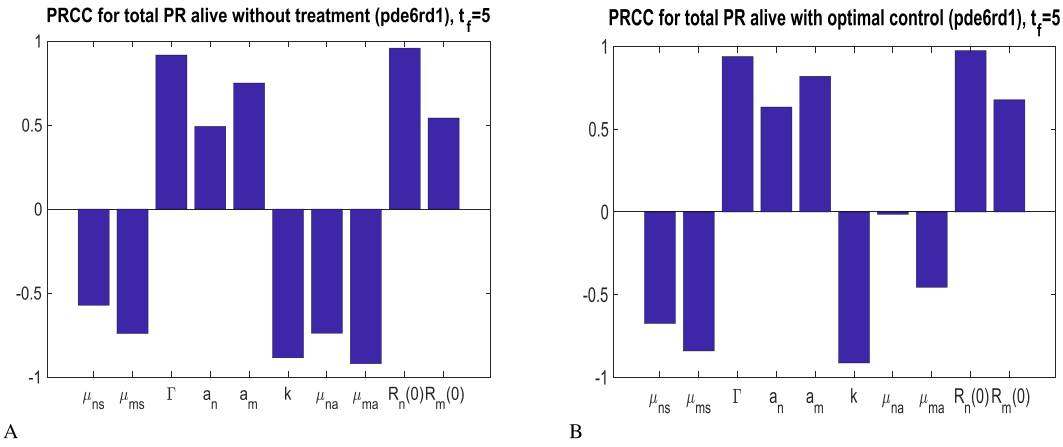

FIG. 3. **PRCC plots without and with optimal control for the $Pde6b^{Rd1}$ mouse model.** The panels, A and B, are the PRCC values for the total PR populations without and with optimal MANF treatment, respectively. In comparing the results without control (A) vs. with optimal control (B), the magnitude of apoptosis in the mutated rods (μ_{ma}) is remarkably lessened and in the normal rods (μ_{na}) is not significant. Thus, treating RP photoreceptors with MANF is very effective in eliminating the effects of apoptosis. Shedding and renewing of OS for rods (μ_{ns}, μ_{ms}, $a_n$and a_m), the nutrient supply (Γ), the limiting characteristics of the nutrients (k) and the initial rod populations ($R_n(0)$ and $R_m(0)$) play an important role in the overall photoreceptor population with non-apoptosis parameters all being the same relative magnitude. Focus areas of treatment should alter these processes as shown in Camacho *et al.* (2016a,b).

In the BALB/cJ mouse model (Fig. 1), focus areas of treatment, both with and without treatment with MANF, should further reduce apoptosis, increase the nutrient supply (Γ), decrease the limiting characteristics of nutrients (k) and maintain a balance in the energy consumption to uptake ratio (μ_{ns}/a_n)

TABLE 2 *Most significant parameters from sensitivity analysis results of mathematical model without and with optimal control. The ↑ indicates that an increase in the given parameter will result in additional photoreceptors surviving at time t_f whereas ↓ indicates that a decrease in the given parameter will result in additional photoreceptors surviving at time t_f. Items not highlighted as 'key differences' are the same relative magnitude*

Mouse model	t_f	Common significant parameters without and with optimal control	Key differences with optimal control vs. without	Figure
BALB/cJ	2 days	$\downarrow \mu_{ns}, \uparrow \Gamma, \uparrow a_n, \downarrow k, \downarrow \mu_{na}, \uparrow R_n(0)$	μ_{ns}, Γ, a_n, k are more significant μ_{na} is less significant	1
C57BL/6	2 days	$\downarrow \mu_{ns}, \uparrow \Gamma, \uparrow a_n, \downarrow k, \downarrow \mu_{na}, \uparrow R_n(0)$	μ_{na} is less significant	2
$Pde6b^{Rd1}$	5 days	$\downarrow \mu_{ns}, \downarrow \mu_{ms}, \uparrow \Gamma, \uparrow a_n, \uparrow a_m,$ $\downarrow k, \downarrow \mu_{na}, \downarrow \mu_{ma}, \uparrow R_n(0), \uparrow R_m(0)$	a_n is more significant, μ_{ma} is less significant, μ_{na} is not significant	3

by either decreasing the rate of OS shedding or increasing the rate of OS renewal and their associated metabolism. In the C57BL/6 mouse model (Fig. 2), focus areas of treatment would be similar to those for BALB/cJ but would potentially require less effort as degeneration in this type of mouse model is slower. In the $Pde6b^{Rd1}$ mouse model (Fig. 3), in which RP is present and photoreceptor degeneration begins approximately on the seventh day after birth, treatment with MANF removes the significance of apoptosis for the normal rods (μ_{na}) and greatly reduces it for the mutated rods (μ_{ma}). Thus, in the presence of MANF, apoptosis is almost insignificant compared with other mechanisms that can further reduce degeneration of photoreceptors; these are the shedding and renewing of OS for rods (μ_{ns}, μ_{ms}, a_n and a_m), the nutrient supply (Γ), the limiting characteristics of the nutrients (k) and the initial rod populations ($R_n(0)$ and $R_m(0)$).

The work of Camacho *et al.* (2016a,b) and Camacho & Wirkus (2013) revealed that increasing the nutrient carrying capacity (Γ/k) and maintaining balanced energy consumption to energy uptake ratios (μ_{is}/a_i, for $i = m, n, c$) can significantly reduce photoreceptor degeneration in RP while the work in Aït-Ali *et al.* (2015), Léveillard & Sahel (2010), Sahel (2005) and Yang *et al.* (2009) showed that the rods are essential for maintaining cones alive by accelerating their glucose uptake via RdCVF. This body of work supports the significance of all these parameters.

Across the three mouse models, the common parameters affecting the nutrient carrying capacity (Γ/k) and the energy consumption to energy uptake ratios are always present. Affecting these parameters in the nutrient carrying capacity has been the focus of numerous experiments as described above. The importance of the balance of the energy consumption to uptake ratios without MANF treatment has previously been suggested (Camacho *et al.*, 2016b; Camacho & Wirkus, 2013), and its significance remains even in the presence of MANF treatment. The key difference in the results of the three mouse models seems to be in the role that apoptosis, and hence MANF treatment, plays. In our PRCC analysis, we have shown that MANF has a significant role in preventing retinal degeneration in all three mouse model and almost eliminates apoptosis in the $Pde6b^{Rd1}$ model.

4.2 *Optimal control in three mouse models*

The sensitivity analysis results demonstrated that apoptosis played the most significant role of all of the mechanisms that can be altered through various treatments in two of the three mouse models (the

TABLE 3 *Summary of mouse models used by and experimental results of Neves et al. (2016). The percentages of surviving photoreceptors predicted by the mathematical model are then compared and the corresponding objective functional values, J, given*

Mouse model	BALB/cJ	C57BL/6	*Pde6b*^{Rd1}
Characteristics of mouse model	high sensitivity to light no mutation	normal sensitivity to light no mutation	RP model mutation present
Methods in Neves experiment to observe apoptosis	exposure to 5klux for 1 hr; measure surviving photoreceptors after 2 days	exposure to 8 klux for 1.5 hrs; measure surviving photoreceptors after 2 days	observe degeneration from day 7 after birth; measure surviving photoreceptors at day 12 after birth
Observed rate of apoptosis	0.65 per day for rods and cones	0.35 per day for rods and cones	0.22 per day for rods only
% photoreceptors surviving w/o treatment at time t_f	[23.1%, 29.2%]	[44.9%, 52.6%]	[35.3%, 37.7%]
% photoreceptors surviving with MANF treatment at time t_f	[51.7%, 56.3%]	[56.2%, 63.5%]	[64.4%, 68.1%]
Math model			
% photoreceptors surviving w/o treatment at time t_f	28.5%	51.6%	36.4%
% photoreceptors surviving with MANF treatment at time t_f	54.6%	62.8%	65.9%
Obj. func. value: $J(u = 0)$	2.16×10^7	2.27×10^7	1.75×10^8
Obj. func. value: $J(u_{\text{opt}})$	2.58×10^7	2.81×10^7	2.12×10^8
Obj. func. value: $J(u = 0.9)$	2.20×10^7	2.19×10^7	1.97×10^8

BALB/cJ model and the C57BL/6 model). Therefore, it is important to explore with specific examples what a MANF-only treatment does to prevent the degeneration of photoreceptors. We note that an overabundance of MANF is experimentally administered in each mouse model so that not all MANF is utilized by the photoreceptors. Without any theoretical or experimental knowledge of toxicity levels of MANF, we assume that the amount of photoreceptors preserved is maximal and thus aim to use our mathematical model to find the minimum dose and strategy of dosing that will replicate these results. Initially, we give a brief discussion of the algorithm solving the optimal control problem and related results in connection with experimental research. Then we present the numerical solutions of the mathematical model under optimal treatment with MANF for the three different mouse models and experiments.

We solve the optimality system (consisting of the state system in (12)–(15), the adjoint system in (20)–(23) and the optimal control characterization in (24)) by the forward-backward sweep method (FBSM) (Lenhart & Workman, 2007). The implementation of the stopping criteria for the FBSM checks the convergence of successive iterates of controls, states and adjoints. For the numerical runs, we choose the weights α_i so that the model output with control matches the experimental observations of the percentage of photoreceptors present at the end of treatment. The relative sizes of the four weights in the objective functional is essential. We set $\epsilon = 1$ and then the values of the other three weights, α_i, were chosen due to their rescue effects (percentage of surviving photoreceptors at the final time) to lie in the corresponding ranges in the experiments. We also set $\alpha_1 = \alpha_2$ because there is no experimental work or evidence suggesting that MANF affects the phenotypic rod types, R_n and R_m, differently. As mentioned earlier, we theoretically assume the control u to take values, $0 \leq u < 1$. For the computations in this section, we let $0.1 \leq u \leq 0.9$. The upper bound is present because no studies have been done indicating the effectiveness of different dosages of MANF in the photoreceptors. Therefore, we assume, arbitrarily, that MANF is at most 90% effective. Analogously, the lower bound is present because experimental evidence suggests that even small levels of MANF have an effect.

In the graphs of the optimal control solutions, Figs 4–6 initially show a small increase in the photoreceptor populations, R_n, R_m and C, before it begins to decrease. We note that fractions of the variables R_n, R_m and C are interpreted as OS discs and thus the variables represent the cumulative number of photoreceptors as measured by both the total number of photoreceptors and respective heights of each. As each photoreceptor height is a delicate balance of renewal at the basal end and shedding at the distal tip and apoptosis directly affects an individual photoreceptor, the brief increase in R_n, R_m and C at the beginning of some of the experiments when control is applied can be interpreted as a small disruption in this balance. Previous work on the non-control equations has shown the presence of limit cycles, interpreted as the rhythmic shedding and renewal of the OS, and thus a brief increase in the non-control output also has a biological interpretation (Camacho *et al.*, 2016c). In all of the graphs of the control function $u(t)$, note that $u(t)$ reaches its bounds. With such bounds imposed, one does not expect to have a smooth curve.

Table 3 summarizes the results of the experiments by Neves *et al.* (2016) and the output of the mathematical model presented here. Figures 4–6 show plots of rods, cones and trophic pool over time for the optimal control, without control ($u = 0$) and for the control fixed at its maximum value ($u = 0.9$). All plots are within the range of the corresponding mouse model experiments; see Table 3.

In terms of our mathematical model, the parameters in equation (26) without control ($u = 0$) give $C^* = R_n^* = R_m^* = 0$, $T^* \neq 0$ as the stable equilibrium. We again note that with optimal control we take into account any potential toxicity associated with excessive treatment and overadministration of MANF. The values of the objective functional for these three different control values ($u = 0$, optimal u and $u = 0.9$) capture this effect, as maximizing the objective functional allows us to achieve high population levels of photoreceptors while not applying excessive treatment.

5. Conclusion

Experimental results suggest that the prominent role played by MANF in preventing photoreceptor degeneration is due to apoptosis. It is thus crucial to have a better understanding of how such treatment affects the system. We modified a mathematical model of photoreceptor degeneration to reflect the role of apoptosis in three experimental mouse models considered in Neves *et al.* (2016) (representing a fast and a slow light sensitive non-disease degeneration models and a diseased retina degeneration

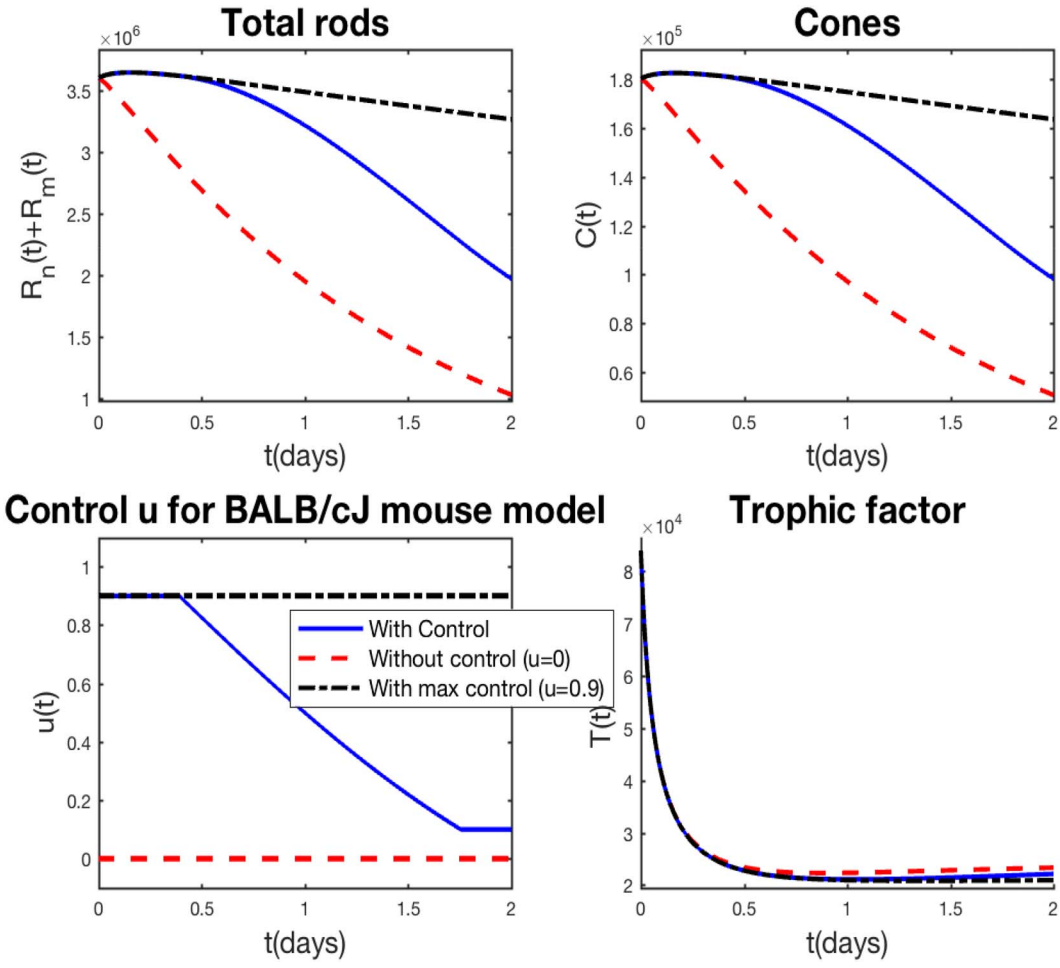

FIG. 4. **BALB/cJ mouse model results with $\varepsilon = 1$, $\alpha_1 = 5$, $\alpha_2 = 5$, $\alpha_3 = 4$ in equation (16)**. Parameters are given in (27) with $\mu_{na} = \mu_{ma} = \mu_{ca} = 0.65$. The objective functional value with optimal control is $J = 2.577 \times 10^7$, without control $J = 2.162 \times 10^7$, and with maximum control ($u = 0.9$) $J = 2.199 \times 10^7$. Each plot shows the results with optimal control, without control ($u = 0$) and with maximal control ($u = 0.9$) for comparison. Top left: total rods vs. time. Top right: cones vs. time. Bottom left: control u vs. time. Bottom right: trophic factor vs. time.

model). We examined the significance of various processes defined by the parameters of the systems with and without MANF treatment as well as the optimal treatment levels for these three mouse models. Our sensitivity analysis results showed the key role of apoptosis in affecting the overall photoreceptor population with and without MANF treatment as well as the significance of the other mechanisms/processes and how their significance is altered with the optimal MANF treatment. Here the optimal treatment is the one given by the optimal control which maximizes the photoreceptors while taking into account potential toxicity from overadministration of MANF, whose potential toxic levels are still unknown. By identifying the most significant parameters and how these affect the population levels of photoreceptors as well as how their significance changes with MANF treatment we can direct clinical

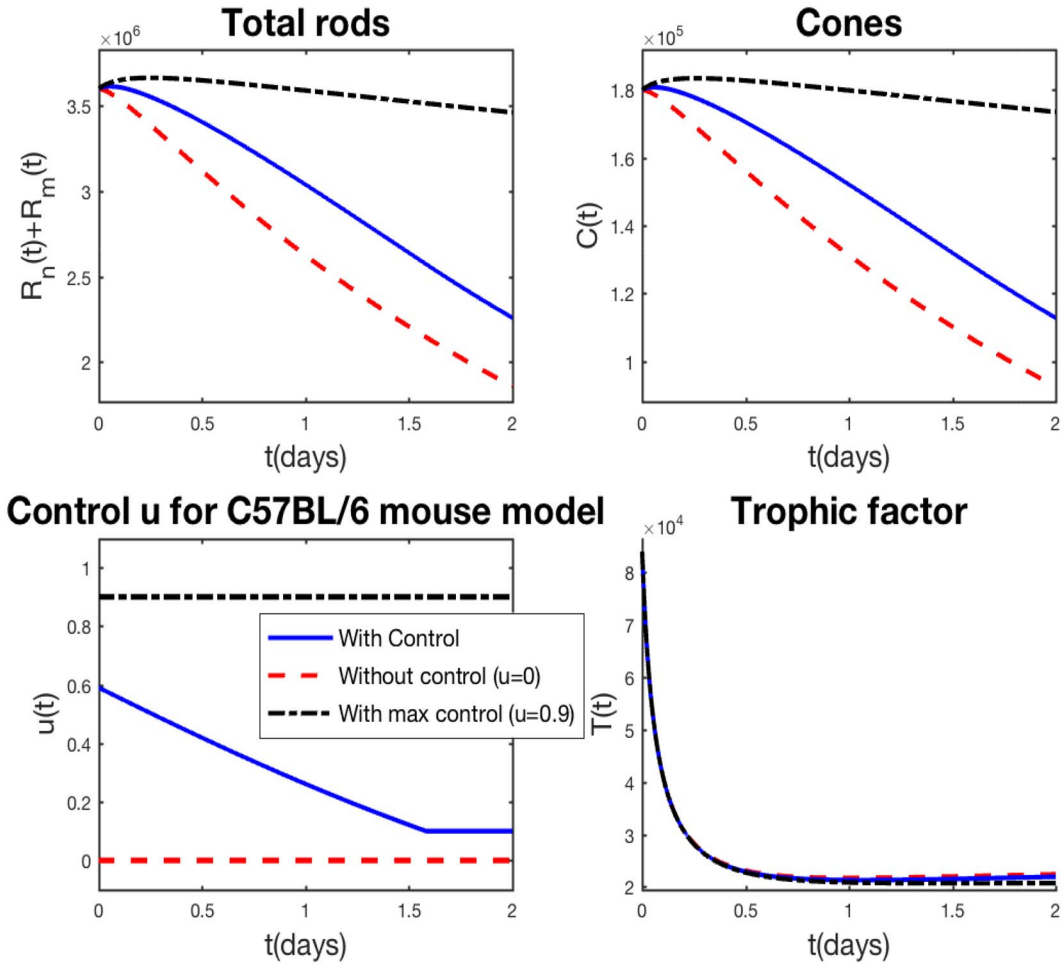

FIG. 5. **C57BL/6 mouse model results with $\varepsilon = 1, \alpha_1 = 5, \alpha_2 = 5, \alpha_3 = 2$ in equation (16).** Parameters are given in (27) with $\mu_{na} = \mu_{ma} = \mu_{ca} = 0.35$. The objective function value with control is $J = 2.883 \times 10^7$, without control $J = 2.724 \times 10^7$, and with maximum control ($u = 0.9$) $J = 2.195 \times 10^7$. Each plot shows the results with optimal control, without control ($u = 0$) and with maximal control ($u = 0.9$) for comparison. Top left: total rods vs. time. Top right: cones vs. time. Bottom left: control u vs. time. Bottom right: trophic factor vs. time.

researchers into potential treatment focus areas. This work gives insight into areas of treatment that can be utilized in conjunction with MANF to magnify their effect of preventing photoreceptor degeneration. For example, in the case of the BALB/cJ mouse model the effect of all significant processes (except for apoptosis) is augmented in the presence of an optimal MANF treatment. In this case, potential treatments that are currently being investigated and that balance energy between consumption and uptake, elimination of any disruptions in shedding and renewal of OS and sufficient nutrient supply (which includes glucose, RdCVF and neuroprotective factors such as PEDF, bFGF and CNTF) can be combined with MANF treatment. (Camacho *et al.*, 2016b; Li *et al.*, 2010; Mohand-Saïd *et al.*, 1998; Mohand-Said *et al.*, 2000, 2001; Punzo *et al.*, Jan 2009, 2012; Strauss, 2005).

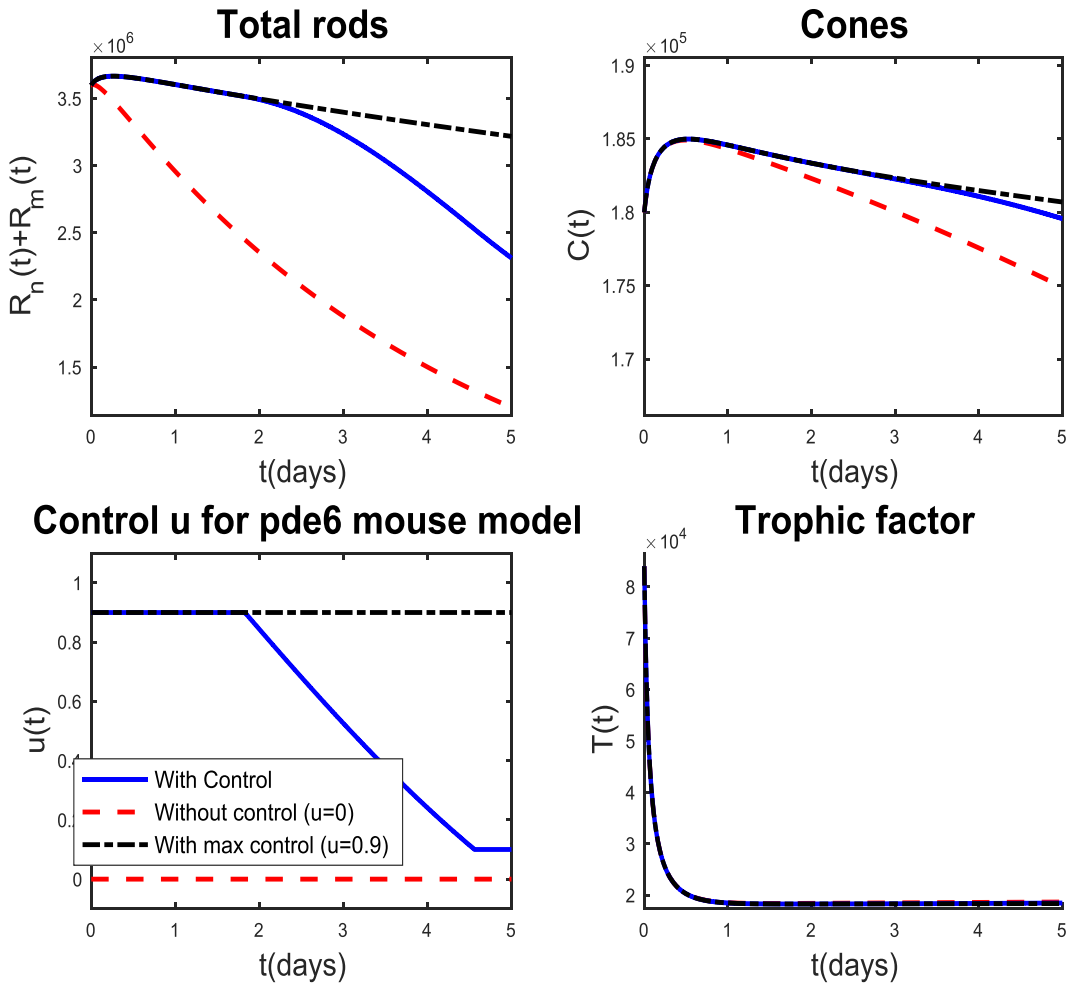

FIG. 6. ***Pde6b*^{Rd1} mouse model results with $\varepsilon = 1$, $\alpha_1 = 15$, $\alpha_2 = 15$, $\alpha_3 = 10$ in equation (16).** Parameters are given in (27) with $\mu_{na} = \mu_{ma} = 0.22$, $\mu_{ca} = 0$. The objective functional value with control is $J = 2.120 \times 10^8$, without control $J = 1.753 \times 10^8$, and with maximum control ($u = 0.9$) $J = 1.970 \times 10^8$. Each plot shows the results with optimal control, without control ($u = 0$) and with maximal control ($u = 0.9$) for comparison. Top left: total rods vs. time. Top right: cones vs. time. Bottom left: control u vs. time. Bottom right: trophic factor vs. time.

With parameter values chosen carefully based on previous work (Camacho *et al.*, 2016b), the initial and final population values from the model simulations of our optimal control model with MANF treatment are in the ranges from experimental observations in Neves *et al.* (2016). Our results confirm the importance of increasing the nutrient carrying capacity (Γ/k) and maintaining balanced energy consumption to energy uptake ratios (μ_{is}/a_i, for $i = m, n, c$) in reducing photoreceptor degeneration in both diseased and non-diseased retinas, as well as the importance of the rods ($R_n(0)$ and $R_m(0)$) in preserving photoreceptors in RP retinas (Aït-Ali *et al.*, 2015; Camacho *et al.*, 2016a,b; Camacho & Wirkus, 2013; Léveillard & Sahel, 2010; Sahel, 2005; Yang *et al.*, 2009). Our control model can be used to guide administration of MANF under various toxicity levels for both disease and light-induced

photoreceptor degeneration. The results of this model suggest that MANF combined with additional targeted treatment areas can be part of a treatment strategy to slow or stop the degeneration of the photoreceptors regardless of the cause.

Acknowledgements

The authors would like to thank the reviewers for their insightful comments and helpful suggestions for improving the readability and presentation of the paper.

References

Aït-Ali, N., Fridlich, R., Millet-Puel, G., Clérin, E., Delalande, F., Jaillard, C., Blond, F., Perrocheau, L., Reichman, S., Byrne, L. C.et al. (2015) Rod-derived cone viability factor promotes cone survival by stimulating aerobic glycolysis. *Cell*, **161**, 817–832.

Berson, E. L. (1993) Retinitis pigmentosa. The Friedenwald Lecture. Retinal photorecptor-pigment epithelium interactions: Friedenwald lecture. *Invest. Ophthalmol. Vis. Sci.*, **34**, 1659–1676.

Besharse, J. & Bok, D. (2011) *The Retina and Its Disorders*. Cambridge, MA: Academic Press.

Bok, D. (1985) Retinal photorecptor-pigment epithelium interactions: Friedenwald lecture. *Invest. Ophthalmol. Vis. Sci.*, **26**, 1659–1694.

Bourne, R. R. A., Flaxman, S. R., Braithwaite, T., Cicinelli, M. V., Das, A., Jonas, J. Keeffe, J., Kempen, J. H., Leasher, J., Limburg, H. *et al.* (2017) Magnitude, temporal trends, and projections of the global prevalence of blindness and distance and near vision impairment: a systematic review and meta-analysis. *Lancet Glob. Health*, **5**, e888–e897.

Busskamp, V., Duebel, J., Balya, D., Fradot, M., Viney, T. J., Siegert, S., Groner, A. C., Cabuy, E., Forster, V., Seeliger, M. *et al.* (2010) Genetic reactivation of cone photoreceptors restores visual responses in retinitis pigmentosa. *Science*, **329**, 413–417.

Camacho, E. T., Colón Vélez, M. A., Hernández, D. J., Rodríguez Bernier, U., van Laarhoven, J. & Wirkus, S. (2010) A mathematical model for photoreceptor interactions. *J. Theor. Biol.*, **21**, 638–646.

Camacho, E. T., Léveillard, T., Sahel, J.-A. & Wirkus, S. (2016a) Mathematical model of the role of rdcvf in the coexistence of rods and cones in a healthy eye. *Bull. Math. Biol.*, **78**, 1394–1409.

Camacho, E. T., Punzo, C. & Wirkus, S. A. (2016b) Quantifying the metabolic contribution to photoreceptor death in retinitis pigmentosa via a mathematical model. *J. Theor. Biol.*, **408**, 75–87.

Camacho, E. T., Radulescu, A. & Wirkus, S. (2016c) Bifurcation analysis of a photoreceptor interaction model for retinitis pigmentosa. *Commun. Nonlinear Sci. Numer. Simul.*, **38**, 267–276.

Camacho, E. T. & Wirkus, S. (2013) Tracing the progression of retinitis pigmentosa via photoreceptor interactions. *J. Theor. Biol.*, **317**, 105–118.

Camacho, E. T., Melara, L. A., Villalobos, M. C. & Wirkus, S. (2014) Optimal control in the treatment of retinitis pigmentosa. *Bull. Math. Biol.*, **76**, 292–313.

Chalmel, F., Léveillard, T., Jaillard, C., Lardenois, A., Berdugo, N., Morel, E., Koehl, P., Lambrou, G., Holmgren, A. *et al.* (2007) Rod-derived cone viability factor-2 is a novel bifunctional-thioredoxin-like protein with therapeutic potential. *BMC Mol. Biol.*, **8**, 74.

Frasson, M., Picaud, S., Léveillard, T., Simonutti, M., Mohand-Saïd, S., Dreyfus, H., Hicks, D. & Sahel, J. (1999) Glial cell line-derived neurotrophic factor induces histologic and functional protection of rod photoreceptors in the rd/rd mouse. *Invest. Ophthalmol. Vis. Sci.*, **40**, 844–856.

Guérin, C. J., Lewis, G. P., Fisher, S. K. & Anderson, D. H. (1993) Recovery of photoreceptor outer segment length and analysis of membrane assembly rates in regenerating primate photoreceptor outer segments. *Invest. Ophthalmol. Vis. Sci.*, **34**, 175–183.

Hamel, C. (2006) Retinitis pigmentosa. *Orphanet J. Rare Dis.*, **1**, 40–51.

Hartong, D. T., Berson, E. L. & Dryja, T. P. (2006) Retinitis pigmentosa. *Lancet*, **368**, 1795–1809.

Hendrickson, A., Bumsted-O'Brien, K., Natoli, R., Ramamurthy, V., Possing, D. and Provis, J. (2008) Rod photoreceptor differentiation in fetal and infant human retina. *Exp. Eye. Res.*, **87**, 415–426.

Jonnal, R. S., Besecker, J. R., Derby, J. C., Kocaoglu, O. P., Cense, B., Gao, W., Wang, Q. & Miller, D. T. (2010) Imaging outer segment renewal in living human cone photoreceptors. *Opt. Express*, **18**, 5257–5270.

Keener, J. & Sneyd, J. (2008) *Mathematical Physiology II: Systems Physiology*. New York, NY: Springer.

Kernan, F. A. G., McKee, G. J. F. & Humphries, P. (2007) On the suppression of photoreceptor cell death in retinitis pigmentosa. *Ophthalmology Research: Retinal Degenerations: Biology, Diagnostics, and Therapeutics*. Totowa, NJ: Humana Press Inc.

LaVail, M. M., Yasumura, D. & Matthes, M. T., Lau-Villacorta, C., Unoki, K., Sung, C.-H. & Steinberg, R. H. (1998) Protection of mouse photoreceptors by survival factors in retinal degenerations. *Invest. Ophthalmol. Vis. Sci.*, **39**, 592–602.

Lenhart, S. and Workman, J. T. (2007) *Optimal Control Applied to Biological Models*. Chapman & Hall/CRC Mathematical and Computational Biology Series. Boca Raton, FL: Chapman and Hall/CRC.

Léveillard, T., Mohand-Saïd, S., Lorentz, O., Hicks, D., Fintz, A.-C., Clérin, E., Simonutti, M., Forster, V., Cavusoglu, N., Chalmel, Dollé, P., Poch, O., Lambrou, G. & Alain Sahel, J. *et al.* (2004) Identification and characterization of rod-derived cone viability factor. *Nat. Genet.*, **36**, 755–759.

Léveillard, T. & Sahel, J.-A. (2010) Rod-derived cone viability factor for treating blinding diseases: from clinic to redox signaling. *Science translational medicine*, **2**, 26ps16–26ps16.

Li, Y., Tao, W., Luo, L., Huang, D., Kauper, K., Stabila, P., LaVail, M. M., Laties, A. M. & Wen, R. (2010) Cntf induces regeneration of cone outer segments in a rat model of retinal degeneration. *PLoS ONE*, **5**, 1–7.

Lindholm, P. & Saarma, M. (2010) Novel cdnf/manf family of neurotrophic factors. *Dev. Neurobiol.*, **70**, 360–371.

Longbottom, R., Fruttigera, M., Douglasb, R. H., Martinez-Barberac, J. P., Greenwooda, J. & Mossa, S. E. (2009) Genetic ablation of retinal pigment epithelial cells reveals the adaptive response of the epithelium and impact on photoreceptors. *Proc. Natl Acad. Sci. U. S. A.*, **3**, 18728–18733.

Malanson, K. M. and Lem, J. (2009) Chapter 1 rhodopsin-mediated retinitis pigmentosa. *Progress in Molecular Biology and Translational Science*. **88**, 1–31.

Marino, S., Hogue, I. B., Ray, C. J. & Kirschner, D. E. (2008) A methodology for performing global uncertainty and sensitivity analysis in systems biology. *J. Theor. Biol.*, **254**, 178–196.

Matsumoto, H., Kataoka, K., Tsoka, P., Connor, K. M., Miller, J. W. & Vavvas, D. G. (2014) Strain difference in photoreceptor cell death after retinal detachment in mice. *Invest. Ophthalmol. Vis. Sci.*, **55**, 4165–4174.

Mohand-Saïd, S., Deudon-Combe, A., Hicks, D., Simonutti, M., Forster, V., Fintz, A.-C., Léveillard, T., Dreyfus, H. & Sahel, J. A. (1998) Normal retina releases a diffusible factor stimulating cone survival in the retinal degeneration mouse. *Proc. Natl. Acad. Sci. U. S. A.*, **95**, 8357–8362.

Mohand-Said, S., Hicks, D., Dreyfus, H. & Sahel, J. A. (2000) Selective transplantation of rods delays cone loss in a retinitis pigmentosa model. *Arch. Ophthalmol.*, **118**, 807–811.

Mohand-Said, S., Hicks, D., Léveillard, T., Picaud, S., Porto, F. & Sahel, J. A. (2001) Rod-cone interactions: developmental and clinical significance. *Prog. Retin. Eye Res.*, **20**, 451–467.

Murakami, Y., Ikeda, Y., Yonemitsu, Y., Onimaru, M., Nakagawa, K., Kohno, R.-I., Miyazaki, M., Hisatomi, T., Nakamura, M., Yabe, T. *et al.* (2008) Inhibition of nuclear translocation of apoptosis-inducing factor is an essential mechanism of the neuroprotective activity of pigment epithelium-derived factor in a rat model of retinal degeneration. *Am. J. Pathol.*, **173**, 1326–1338.

Murakami, Y., Matsumoto, H., Roh, M., Suzuki, J., Hisatomi, T., Ikeda, Y., Miller, J. W. & Vavvas, D. G. (2012) Receptor interacting protein kinase mediates necrotic cone but not rod cell death in a mouse model of inherited degeneration. *Proc. Natl. Acad. Sci. U. S. A.*, **109**, 14598–14603.

Neves, J., Zhu, J., Sousa-Victor, P., Konjikusic, M., Riley, R., Chew, S., Qi, Y., Jasper, H. & Lamba, D. A. (2016) Immune modulation by manf promotes tissue repair and regenerative success in the retina. *Science*, **353**, aaf3646.

Oyster, C. W. (1999) *The Human Eye: Structure and Function*. Sunderland, MA: Sinauer Associates, Inc.

Pallikaris, A., Williams, D. R. & Hofer, H. (2003) The reflectance of single cones in the living human eye. *Invest. Ophthalmol. Vis. Sci.*, **44**, 4580–4592

Papermaster, S. D. (2002) The birth and death of photoreceptors: the friedenwald lecture. *Invest. Ophthalmol. Vis. Sci.*, **43**, 1300–1309.

Petrova, P. S., Raibekas, A., Pevsner, J., Vigo, N., Anafi, M., Moore, M. K., Peaire, A., Shridhar, V., Smith, D. I., Kelly, J. et al. (2004) Discovering novel phenotype-selective neurotrophic factors to treat neurodegenerative diseases. *Prog. Brain Res.*, **146**, 167–183.

Phelan, J. K. & Bok, D. (2000) A brief review of retinitis pigmentosa and the identified retinitis pigmentosa genes. *Mol. Vis.*, **6**, 116–124.

Pizzarello, L., Abiose, A., Ffytche, T., Duerksen, R., Thulasiraj, R., Taylor, H., Faal, H., Rao, G., Kocur, I. & Resnikoff, S. (2004) Vision 2020: The right to sight: a global initiative to eliminate avoidable blindness. *Arch. Ophthalmol.*, **122**, 615–620.

Pontryagin, L. S. (2018) *Mathematical Theory of Optimal Processes*. Abingdon-on-Thames, United Kingdom: Routledge.

Punzo, C., Kornacker, K. & Cepko, C. L. (2009) Stimulation of the insulin/mtor pathway delays cone death in a mouse model of retinitis pigmentosa. *Nat. Neurosci.*, **12**, 44–52.

Punzo, C., Xiong, W. & Cepko, C. L. (2012) Loss of daylight vision in retinal degeneration: are oxidative stress and metabolic dysregulation to blame? *J. Biol. Chem.*, **287**, 1642–1648.

Sahel, J.-A. (2005) Saving cone cells in hereditary rod diseases: a possible role for rod-derived cone viability factor (rdcvf) therapy. *Retina*, **25**, S38–39.

Shen, J., Yang, X., Dong, A., Petters, R. M., Peng, Y.-W., Wong, F. & Campochiaro, P. A. (2005) Oxidative damage is a potential cause of cone cell death in retinitis pigmentosa. *J. Cell. Physiol.*, **203**, 457–464.

Shintani, K., Shechtman, D. L. & Gurwood, A. S. (2009) Review and update: current treatment trends for patients with retinitis pigmentosa. *Optometry*, **80**, 384–401.

Strauss, O. (2005) The retinal pigment epithelium in visual function. *Physiol. Rev.*, **85**, 845–881.

Wenzel, A., Grimm, C., Samardzija, M. & Remé, C. E. (2005) Molecular mechanisms of light-induced photoreceptor apoptosis and neuroprotection for retinal degeneration. *Prog. Retin. Eye Res.*, **24**, 275–373.

Wenzel, A. Reme, E.C., Williams, P. T., Hafezi, F. and Grimm, C. (2001) The rpe65 leu450met variation increases retinal resistance against light-induced degeneration by slowing rhodopsin regeneration. *J. Neurosci.*, **21**, 53–58.

Wong, F. (1997) Investigating retinitis pigmentosa: a laboratory scientist's perspective. *Prog. Retin. Eye Res.*, **16**, 353–373.

World Health Organization Vision Impairment and Blindness (2017) Vision Impairment and Blindness. Fact sheet, updated October 2017, https://www.who.int/news-room/fact-sheets/detail/blindness-and-visual-impairment.

World Health Organization Vision Media Center (2018) Blindness: Vision 2020—the global initiative for the elimination of avoidable blindness. Fact sheet no. 213, https://www.who.int/mediacentre/factsheets/fs213/en/ .

Yang, Y., Mohand-Said, S., Danan, A., Simonutti, M., Fontaine, V., Clerin, E., Picaud, S., Léveillard, T. & Sahel, J.-A. (2009) Functional cone rescue by RdCVF protein in a dominant model of retinitis pigmentosas. *Mol. Ther.*, **17**, 787–795.

Young, R. (1971) The renewal of rod and cone outer segments in the rhesus monkey. *J. Cell Biol.*, **49**, 303–318.